Macropinocytosis: regulated coordination of endocytic and exocytic membrane traffic events

Sestina Falcone[1,2,*], Emanuele Cocucci[3,*], Paola Podini[2], Tomas Kirchhausen[4], Emilio Clementi[1,2] and Jacopo Meldolesi[2,3,5,‡]

[1]University of Milan, Department of Preclinical Sciences, via G.B. Grassi 74, 20157 Milan, Italy, and E. Medea Scientific Institute, 23842 Bosisio Parini, Italy
[2]Scientific Institute San Raffaele, Stem Cell Research Institute and [3]Vita-Salute San Raffaele University, Department of Neuroscience, Center of Excellence on Cell Development, via Olgettina 58, 20132 Milan, Italy
[4]Harvard Medical School, The CBR Institute for Biomedical Research, Longwood Avenue, Boston, MA 02115, USA
[5]IIT Research Unit of Molecular Neuroscience, via Olgettina 58, 20132 Milan, Italy

*These authors have contributed equally to this work
‡Author for correspondence (e-mail: meldolesi.jacopo@hsr.it)

Accepted 31 August 2006
Journal of Cell Science 119, 4758-4769 Published by The Company of Biologists 2006
doi:10.1242/jcs.03238

Summary

Macropinocytosis, a form of bulk uptake of fluid and solid cargo into cytoplasmic vacuoles, called macropinosomes, has been studied mostly in relation to antigen presentation. Early membrane traffic events occurring in this process are, however, largely unknown. Using human dendritic cells we show that a marked increase in the rate of macropinocytosis occurs a few minutes after application of two markers (small latex beads or dextran), depends on a slow intracellular Ca2$^+$ concentration ($[Ca^{2+}]_i$) rise that precedes the PI3K-dependent step, and is preceded and accompanied by exocytosis of enlargeosomes compensating in part for the macropinocytic plasma membrane internalization. Unexpectedly, macropinosomes themselves, which share markers with endosomes, undergo Ca^{2+}-dependent exocytosis so that, after ~20 minutes of continuous bead or dextran uptake, an equilibrium is reached preventing cells from overloading themselves with the organelles. Large $[Ca^{2+}]_i$ increases induced by ionomycin trigger rapid (<1 minute) exocytic regurgitation of all macropinosomes, whereas endosomes remain apparently unaffected. We conclude that, in dendritic cells, the rate of macropinocytosis is not constant but increases in a regulated fashion, as previously shown in other cell types. Moreover, macropinosomes are not simple containers that funnel cargo to an endocytic pathway, but unique organelles, distinct from endosomes by their competence for regulated exocytosis and other membrane properties.

Supplementary material available online at
http://jcs.biologists.org/cgi/content/full/119/22/4758/DC1

Key words: Macropinocytosis, Regulated exocytosis, Membrane traffic, Dendritic cells, Enlargeosomes

Introduction

Macropinocytosis is a form of endocytosis taking place in many types of cell. In this process, bending of single surface lamellipodia, giving rise to circular (or curved) ruffles, is followed by sealing of the aperture with formation of discrete vacuoles, the macropinosomes, which are accumulated within the cell (Swanson and Watts, 1995; Steinman and Swanson, 1995). By this paradigm the cell is able to internalize, in bulk, considerable volumes of extracellular fluid and to efficiently take up dissolved molecules as well as particles such as viruses (Pelkmans and Helenius, 2003; Meier and Greber, 2004), bacteria (Kolb-Maurer et al., 2002; Terebiznik et al., 2002) apoptotic cell fragments (Fiorentini et al., 2001; Henson et al., 2001) and also small latex beads (Bds) (Reece et al., 2001; Kolb-Maurer et al., 2002).

In immature dendritic cells (DCs) macropinocytosis has attracted considerable attention because it supports the uptake of antigens destined to appear on the surface (antigen presentation) after long intracellular transport, proteolytic processing and mounting of peptides onto the major histocompatibility complex II (MHCII) (Steinman and Swanson, 1995; West et al., 2004; Sallusto et al., 1995; Mellman and Steinman, 2001; Lutz et al., 1997). Uptake of macropinocytic tracers is known to take place in unstimulated DCs. Based on this, the process is widely (see Sallusto et al., 1995; Swanson and Watts, 1995; Amyere et al., 2002), but not unanimously (West et al., 2004) believed to operate at a constant rate. In other cells, however, such as macrophages, lymphocytes, fibroblasts and epithelial cells, ruffling and generation of macropinosomes increases in rate following application of a variety of stimuli inducing activation of growth factor receptors (Hamasaki et al., 2004; Lanzetti et al., 2004), non-receptor tyrosine kinases (Amyere et al., 2000; Amyere et al., 2002), p21-activated kinase1 (Dharmawardhane et al., 2000; Yang et al., 2005), protein kinase C (Meier and Greber, 2004; Kruth et al., 2005) and small G proteins (Amyere et al., 2002; Lanzetti et al., 2004; Garrett et al., 2000; West et al., 2000; Sun et al., 2003; Ellerbroek et al., 2004; Schnatwinkel et al., 2004; Kruth et al., 2005). Whether macropinocytosis occurring in DCs (constitutive) is distinct from that occurring in other cells types (regulated) has yet to be established.

The two steps of the macropinocytic pathway that have thus

far been studied in detail are macropinosome sealing, with its concomitant dynamic restructuring of the actin cytoskeleton (West et al., 2004; Lanzetti et al., 2004; Kruth et al., 2005; Araki et al., 1996; Araki et al., 2003; Salter et al., 2004; Swanson et al., 1999; Rupper et al., 2001), and late trafficking of antigens to MHCII-positive vacuoles, up to their transport to the cell surface (Mellman and Steinman, 2001; Racoosin and Swanson, 1993; Harding and Geuze, 1992). Less attention has been devoted to processes taking place between the very early and late steps, in particular to the membrane events that follow the generation of macropinosomes and precede their funnelling into an endocytic pathway (see de Baey and Lanzavecchia, 2000; Schnatwinkel et al., 2004; Hamasaki et al., 2004). There are several questions that remain open, including the following: is the generation of macropinosomes controlled by intracellular signals? After their generation, do macropinosomes integrate into the endosomal compartment or do they maintain a functional specificity? Is their lumenal cargo targeted in all cases to its intracellular pathway or can it be regurgitated back into the extracellular space? In this case, is the latter process regulated? And by which intracellular signal?

In the present work, macropinosome membrane traffic events have been investigated in human monocyte-derived DCs maintained for 0.5-30 minutes in continuous contact with fluorescent, fluoresceine isothiocyanate (FITC)- or tetrarhodamine isothiocyanate (TRITC)-coupled tracers: either small latex Bds, 20 nm in diameter, or 70 kDa dextran (Dex). Both these tracers, which are mostly specific for macropinocytosis, are considered to be inert, unable to induce the generation of intracellular messengers. However, their effects on cellular Ca^{2+} homeostasis and the role of Ca^{2+} in their uptake, and intracellular traffic, has never been investigated. By using a fura-2 assay of the cytosolic Ca^{2+} concentration, $[Ca^{2+}]_i$, with a $[Ca^{2+}]_i$ buffering agent and a Ca^{2+} ionophore, together with several drugs active at specific membrane traffic events, we have shown that administration of either tracer is followed by a slow $[Ca^{2+}]_i$ rise. This rise is necessary to substantially increase the rate of their uptake by macropinocytosis; and that recently generated macropinosomes might not only proceed to their intracellular pathway but also be regurgitated by $[Ca^{2+}]_i$-dependent exocytosis.

Results

Intracellular distribution of macropinocytized tracers

Human DCs were exposed to two FITC-conjugated tracers considered inert, i.e. unable to trigger intracellular generation of signals, for 0.5-30 minutes: either small latex beads (20 nm

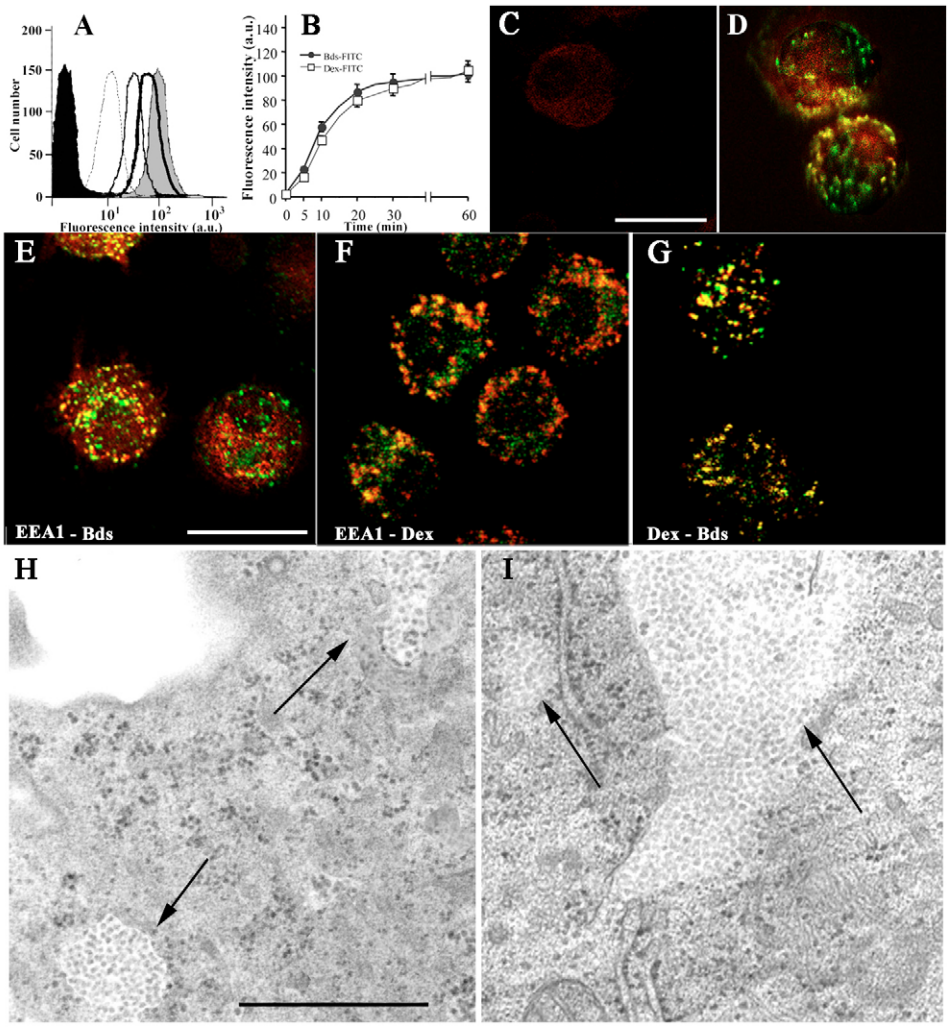

Fig. 1. Tracer and subcellular marker distribution in DC macropinosomes. Panel A shows the accumulation of FITC latex Bds into DCs, revealed by FACS histograms of cell preparations incubated with the tracer, from left to right, for 0, 5, 10, 20 and 60 minutes. The conversion in time-dependent curves of the FACS data, obtained in three experiments with either Bds or Dex, is shown in panel B. Panels C and D show merged confocal images of DCs exposed for 10 minutes to the styryl dye FM4-64 (red), alone (C) or together with FITC-conjugated Bds (green, D). The almost complete negativity of C shows that without the Bds endocytosis is weak, whereas with the Bds the labelled puncta are numerous, mostly positive for both the dye and the tracer (yellow). The merged images of panels E and F show the two tracers (green), Bds (E) and Dex (F), administered for 10 minutes, localized mostly in a fraction of the puncta positive for the early endosome marker EEA1 (red). Panel G illustrates the co-localization of Bds and Dex administered together for 10 minutes to DCs. Bar, 10 μm (C), also valid for D. Bar, 10 μm (E), also valid for F and G. Panels H and I show the ultrastructure of two cytoplasmic areas in DCs loaded with Bds for 10 minutes. Vacuoles of variable size and shape packed with the tracer (macropinosomes) are indicated by arrows. Bar, 0.5 μm (H).

in diameter; hereon referred to as the Bds), which in contrast to Bds of diameter >100 nm are known to be mostly taken up by macropinocytosis and not by phagocytosis (Reece et al., 2001); or the classical macropinocytic tracer, 70 kDa Dex. Cells were then analyzed by FACS, confocal and electron microscopy.

Fig. 1A,B illustrates the accumulation of the two tracers into DCs incubated at 37°C, as revealed by FACS. In both cases little uptake was seen during the first 5 minutes. Thereafter the process became faster, reaching apparent saturation after ~20 minutes (Fig. 1B). In confocal images of 10 minute-loaded cells the tracers appeared concentrated in distinct puncta of various apparent size (0.5-1.5 μm), scattered throughout the cytoplasm (Fig. 1E-G; supplementary material Fig. S1A-F). To establish whether these puncta were membrane patches in continuity with the cell surface or discrete intracellular organelles we used styryl dyes of the FM family, which markedly increase their fluorescence when dissolved into membranes (Cochilla et al., 1999; van der Wijk et al., 2003). In DCs exposed to FM4-64 for 10 minutes, with the tracers (Fig. 1D) or without the tracers (Fig. 1C), the two washes in KRH medium at 4°C induced the release of all surface fluorescence but failed to affect the fluorescence of most puncta rich of Bds (Fig. 1D) or of Dex (not shown), as expected for intracellular organelles. To quantify the process we compared preparations loaded with Bds, before and after washing (three groups of ten cells each). FM positivity was found to persist in over 80% of the puncta. Analogous results were obtained with Dex (not shown).

The nature of the organelles loaded with the tracers was then investigated. Fig. 1E,F shows representative confocal images of DCs which, after loading for 10 minutes with Bds or Dex, were immunolabelled for the early endosomal marker, EEA1. In three groups of ten cells, both Bd-rich (Fig. 1E) and Dex-rich (Fig. 1F) puncta were positive mostly for EEA1 (84±12% and 68±15%, respectively). Many additional EEA1-positive puncta were negative for the tracers. Although the puncta labelled by the two tracers appeared often not to be identical to each other (compare Fig. 1E with Fig. 1F), their nature was most likely the same. In fact, when the two tracers were administered together, they co-localized in the same puncta (Fig. 1G). Some of the puncta positive for the tracers were positive also for the recycling endosome marker, transferrin receptor (TfR): 31±9% and 27±13% for Bds and Dex, respectively (supplementary material Fig. S1A,C). With the lysosomal marker Lamp1 (supplementary material Fig. S1B,D) and with markers of other structures, the endoplasmic reticulum (ER) (calreticulin) and the MHC II-rich vesicles (HLA-DR) (supplementary material Fig. S1E,F), co-labelling of tracers remained below background, as defined by Cocucci et al. (Cocucci et al., 2004).

The ultrastructure of the Bd-rich organelles is shown in Fig. 1H,I. Vacuoles variable in size (profiles from 0.2 μm to a few μm in diameter) and shape (from roughly spherical to highly irregular), packed with Bds (~20 nm in diameter; average density in ten vacuoles: 1220±175 per μm^2), were seen scattered throughout the cytoplasm, adjacent to classical organelles where Bds were never seen. Membrane continuities of these vacuoles with the plasma membrane were observed, albeit very rarely.

The time course of Bd uptake and of Bd or Dex co-localization with organelle markers, quantified by morphometric analysis of confocal images from cells incubated for 0.5-15 minutes, are shown in Fig. 2 and in supplementary material Fig. S2A,B. Corresponding images with Bds and Dex appear in supplementary material Fig. S2C-E. In unwashed preparations, the tracers already appeared in contact with the cells at the earliest time point (not shown). Yet, as previously shown in Fig. 1A,B, the rate of Bd uptake

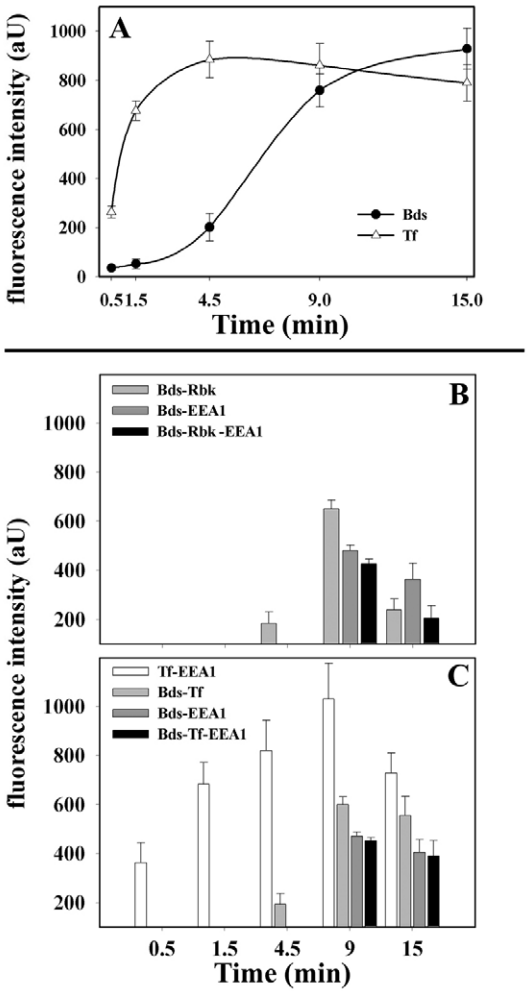

Fig. 2. Kinetics of transferrin and latex bead uptake in DCs immunolabelled for macropinosome-endosome markers: rabankyrin-5 and EEA1. This figure shows quantitative morphometric results (mean ± s.d. from at least ten fields each), obtained as described in Materials and Methods. Corresponding representative images and additional quantitative data with Dex and Bds are shown in supplementary material Fig. S2. Panel A compares the kinetics of uptake by DCs of two tracers, Tf and Bds, taken up by clathrin-dependent endocytosis and macropinocytosis, respectively. Notice that the first appears monophasic, whereas the second shows a considerable increase in rate after a few minutes of delay. Panel B illustrates the time course of Bd accumulation in puncta positive also for Rbk, EEA1 or both; panel C shows the accumulation of Tf in puncta positive for EEA1, and of Bds in puncta positive for Tf, EEA1 or both. Notice that the macropinocytic tracer becomes co-localized with the markers with a few minutes' delay with respect to Tf; and that its co-localization with the two markers is sequential: first Rbk-5 (newly generated macropinosomes and an early endosome subfraction), and then EEA1 (early endosomes).

was initially low but then increased, becoming severalfold higher after 4.5 minutes (Fig. 2A). As a reference, the kinetics of the macropinocytic markers was compared with that of transferrin (Tf), which is also endocytized, although by clathrin-dependent endocytosis. In our experimental conditions, Tf was found to be taken up at a high rate from the start of incubation (Fig. 2A,C). Co-localization of Tf with EEA1 was already considerable at 0.5 minutes and increased thereafter (Fig. 2C). By contrast, co-localization of Bds with organelle markers became appreciable only at 4.5 minutes, and involved Rbk [a marker of macropinosome and early endosome subpopulations (Schnatwinkel et al., 2004)] but not yet EEA1 (Fig. 2B). Co-localization of Bds with EEA1 was considerable at 9 minutes (42±6% of the EEA1-labelled puncta) and declined slightly at 15 minutes (Fig. 2B,C). Bds co-labelling with TfR was also evident, although lower and delayed with respect to that with EE1 (supplementary material Fig. S2A). By contrast, co-labelling of Dex with Rbk and EE1 was similar to that of Bds, as shown in supplementary material Fig. S2B. Finally, co-labelling with non-endosomal markers, Lamp1, calreticulin or HLA-DR, always remained below background (not shown).

We conclude that the rate of macropinocytosis is not stable but increases considerably, starting a few minutes after application of the tracers. Shortly thereafter the macropinosome puncta become positive for EEA1, accounting for almost half of the puncta positive for this endosomal marker. The organelles negative for Bds or Dex do not seem to participate in the initial 30 minutes of macropinosome traffic.

Regulation of macropinocytosis: role of $[Ca^{2+}]_i$

Numerous enzymes and regulatory proteins have been reported to play a key role in macropinosome generation or processing: small G proteins, Rho (Kruth et al., 2005), Rah (Sun et al., 2003), and Rac and Rab-5 (Lanzetti et al., 2004; Schnatwinkel et al., 2004); a few kinases, including srk (Amyere et al., 2000), PAK1 (Dharmawardhane et al., 2000; Yang et al., 2005), and PKC (Muro et al., 2003; Kruth et al., 2005); and phospholipase C (Amyere et al., 2000). In our DCs (Fig. 3), blocking of PI3 kinase (PI3K) by specific inhibitors, such as wortmannin (Wort) (Fig. 3D) and LY-294002 (Fig. 3E) (the inactive analogue LY-303511 had no effect, Fig. 3F), confirmed the requirement of this enzyme (Amyere et al., 2000; Mellman and Steinman, 2001; Racoosin and Swanson, 1993; Araki et al., 2003; Swanson et al., 1999; Rupper et al., 2001). Blockade by the latter drugs is not sufficient for the identification of macropinocytosis because PI3K is also needed for other forms of endocytosis, including the clathrin-dependent form (supplementary material Fig. S3A). Macropinocytosis is also blocked by amiloride, the inhibitor of the Na^+/H^+ exchanger (Fig. 3B) (West et al., 1989; Meier et al., 2002). This result provides an additional criterion, allowing macropinocytosis to be distinguished from phagocytosis and various forms of endocytosis, dependent on either clathrin (supplementary material Fig. S3B) or rafts (not shown), which are unaffected by amiloride (Geckle et al., 2001; Meier et al., 2002; Wadia et al., 2004).

Whether Ca^{2+} is also involved in the regulation of macropinocytosis has never been investigated. Fig. 3G,H shows that application of Bds or Dex to DCs induces a slow and progressive rise of $[Ca^{2+}]_i$, reaching an average of $\Delta R/R_o$ values (R_o being the fura-2 340/380 excitation ratio of resting DCs) ~25% and ~15% above resting levels, in 5 minutes (Fig. 3I). Thereafter these values remained elevated, up to the end of the experiment (30 minutes). The Bd-induced $[Ca^{2+}]_i$ rise was unaffected by cell pretreatment with Wort (documenting its independence from PI3K) or with another drug, vacuolin 1 (Vac1), which

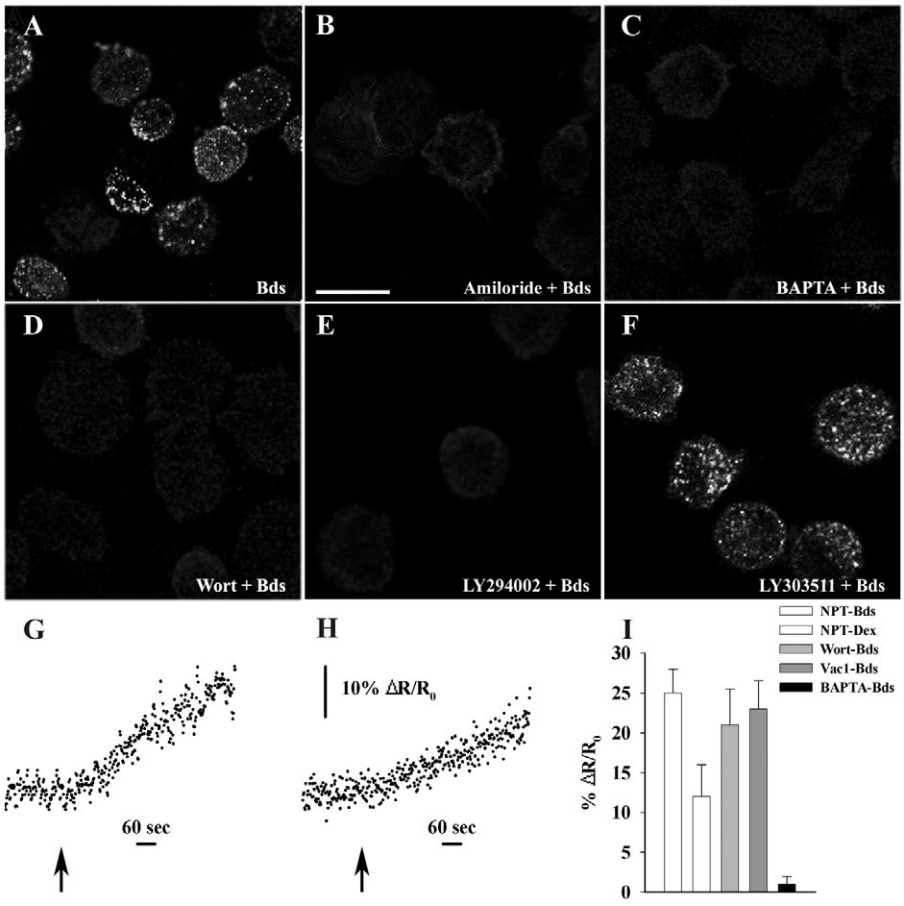

Fig. 3. Macropinosome generation: dependence on PI3K and Ca^{2+}, and effects of tracers on $[Ca^{2+}]_i$. Panels A-B show DCs loaded with Bds without pretreatments (A), after pretreatment with amiloride (B), after preloading with BAPTA (C), and after pretreatment with the PI3K-blocker drugs Wort (D) and LY-294002 (E) or the inactive analogue LY-303511 (F). Bar, 10 μm (B), also valid for A-D. Panels G and H show representative fura-2 ratiometric $[Ca^{2+}]_i$ traces of DC suspensions exposed at the arrows to non-fluorescent Bds (G) or Dex (H). Panel I summarizes the average increases (results of four experiments ± s.d.) induced by the 5 minute addition of either tracer to DCs non-pretreated (NPT) or exposed for the same time to Bds after pretreatment with Wort, Vac1 or BAPTA-AM.

induces swelling of endosomes and lysosomes (Cerny et al., 2004; Huynh and Andrews, 2005) (Fig. 3I). However, when DCs were preloaded with the Ca^{2+} chelator, BAPTA, which buffers the rise of $[Ca^{2+}]_i$ extensively, the macropinocytic uptake of Bds was almost completely blocked (Fig. 3C,I). We conclude that, in Dcs not only PI3K activity, but also the slow rise of $[Ca^{2+}]_i$ induced by the tracers is required for macropinocytosis to take place.

Macropinosomes are discharged by a Ca^{2+}-dependent process

The results shown in Figs 1 and 2 document the macropinocytic uptake of both Bds and Dex, which undergo apparent changes at 4-5 minutes, when the rate increases, and after 20 minutes, when the rate declines to low values. The latter effect could be the consequence of either a real decline of macropinocytosis or of its coupling to a form of exocytic recycling. Other forms of endosomes are known to undergo extensive, but constitutive recycling (Maxfield and McGraw, 2004; Knight, 2002). A few previous studies, conducted in cells other than DCs, have suggested that macropinosomes are also recycled (Veithen et al., 1998; Hamasaki et al., 2004). The regulation of this process had never been studied in detail.

To investigate whether Ca^{2+}-induced exocytosis takes place in DCs, we used a ionophore, ionomycin (IONO) (3 μM), which induces the fura-2 excitation wavelength ratio ($\Delta R/R_o$) to rise promptly to values much higher than those induced by Bds and Dex (compare Fig. 4A,B with Fig. 3E,F). When recalculated in terms of $[Ca^{2+}]_i$ (Cocucci et al., 2004), the rise following the 1-minute application of IONO was found to correspond to a few μM. This rise was unaffected by cell pretreatment with Wort or Vac1 but was almost completely inhibited by BAPTA (Fig. 4B). At a later time point, some $[Ca^{2+}]_i$ rise occurred in BAPTA-loaded cells also, remaining, however, below the value of cells treated with IONO alone (not shown). IONO induced rapid fluorescence increases (+15±0.8%, average of four experiments) in cell preparations incubated in the presence of FM1-43 (Fig. 4C). This finding is indicative of a proportional enlargement of the membrane that, during the experiment, had established direct contact with the extracellular medium. This is a typical consequence of intense exocytic responses. The increases of FM1-43 were significantly inhibited by Wort and, even more, by Vac1 (–38% and –63%, respectively, after a 1-minute application of IONO). Moreover, they were Ca^{2+}-dependent because they were almost completely inhibited by BAPTA (Fig. 4D).

The possible participation of macropinosomes in the IONO-induced exocytic responses was investigated in DCs loaded for 10 minutes with Bds and then exposed to the ionophore. As shown in Fig. 5A-E, within the first minute of application, IONO induced an almost complete disappearance of the Bd-rich, EEA1-positive puncta revealed by fluorescence (–91±5%, average of 20 cells; $P<0.001$; Fig. 5A-C) and of the corresponding Bd-filled vacuoles revealed by electron microscopy (compare Fig. 5E with Fig. 5D). By contrast, the complement of early endosomes free of Bds, revealed by Bd-negative, EEA1-positive puncta, remained considerable (Fig. 5B). We conclude that the rise of $[Ca^{2+}]_i$ induced by IONO triggers the rapid disappearance of macropinosomes, including those positive for EEA1, probably as a consequence of their regulated exocytosis. By contrast, the endosomes, although positive for the same marker, remain apparently unaffected.

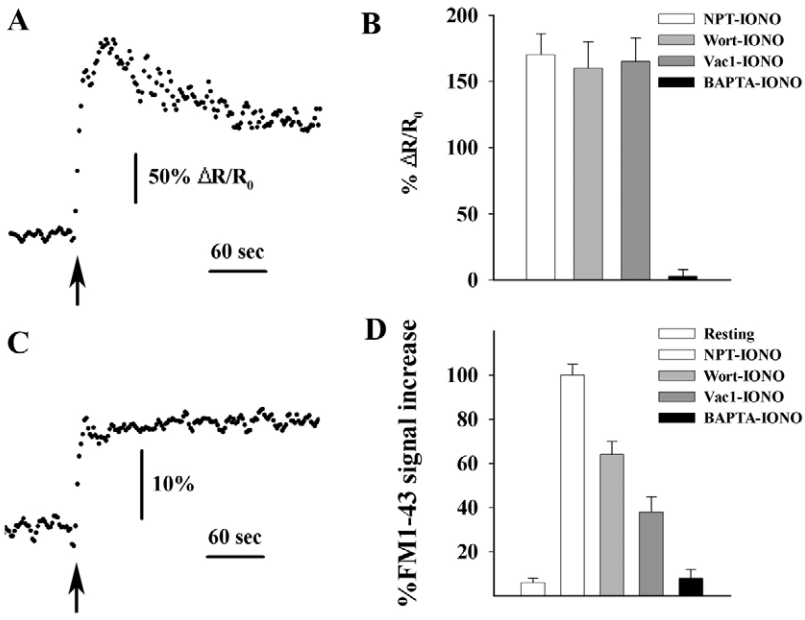

Fig. 4. Effects of ionomycin on DCs: $[Ca^{2+}]_i$ increase and surface area expansion. Panel A shows the increase of the fura-2 ratiometric $[Ca^{2+}]_i$ signal in a DC suspension exposed to IONO (arrow). The average increases at 1 minute (results of four experiments ± s.d.) in DCs, non-pretreated (NPT) and pretreated with Wort, Vac1 or BAPTA-AM, are shown in B. Panel C shows the prompt IONO-induced (arrow) increase of FM1-43 fluorescence recorded in a DC suspension analyzed in the presence of the dye, documenting cell surface expansion; panel D shows the average 1 minute FM1-43 fluorescence increases in DC suspensions pretreated as in panel B (results of four experiments ± s.d.).

Macropinosome exocytosis is inhibited by Vac1

Vac1 is a drug described by Cerny et al. (Cerny et al., 2004) as a blocker of lysosome-regulated exocytosis (see Huynh and Andrews, 2005). Here, we investigated whether, in the experimental conditions specified by Cerny et al. (Cerny et al., 2005), Vac1 does inhibit the IONO-induced discharge of macropinosomes from 10 minute-loaded DCs. In unstimulated cells, Vac1 had no inhibitory effect on Bd accumulation into puncta. Compared with those of untreated cells (Fig. 5A), however, these puncta appeared swollen (Fig. 6A), accounting for a larger fraction of the EEA1-positive puncta (almost 80% versus 45%, $P<0.01$, compare Fig. 6D with Fig. 5C). Lamp1-positive puncta, which appeared also somewhat swollen, exhibited no co-localization with the Bds (Fig. 6C). At the ultrastructural level (Fig. 6E), Vac1-treated DCs appeared full of large vacuoles containing Bds that looked spread out, either loosely or in clusters (average density in ten vacuoles: 525±275 per μm^2 equals 43% of the density of

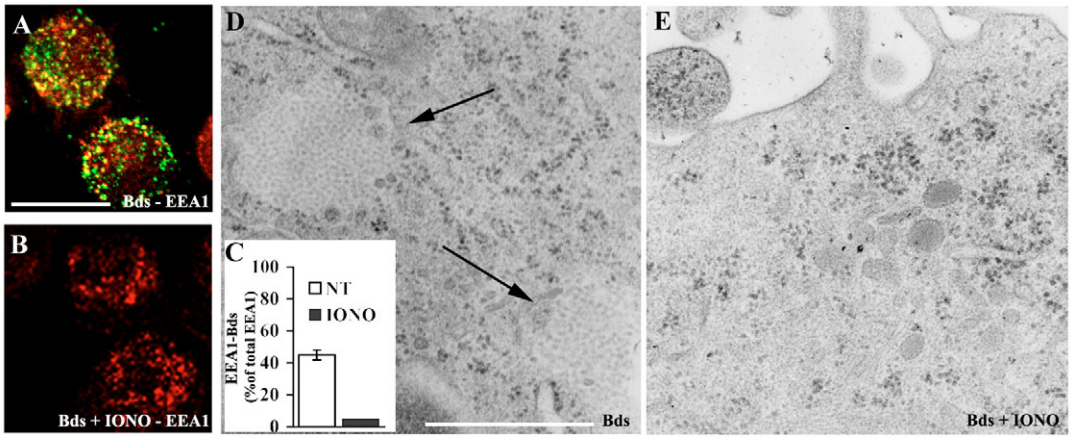

Fig. 5. Ionomycin-induced discharge of macropinosomes. Panel A shows the confocal merged images of DCs loaded for 10 minutes with Bds (green) before fixation, followed by EEA1 immunolabelling (red). The large co-localization of Bds and EEA1 (yellow) is similar to that in Fig. 1E. Panel B shows DCs as in A, but exposed for 1 minute to IONO before fixation and EEA1 immunolabelling. Notice the complete disappearance of the Bds-positive puncta with apparent no change in the puncta positive for EEA1 alone. Bar, 10 μm (A), also valid for B. Panel C shows mean ± s.d. of results on Bd-EEA1-positive puncta such as those in A and B, quantified morphometrically in at least ten fields. Notice that the Bd-EEA1-positive puncta, which before IONO were almost 45% of the whole EEA1-positive population, dropped to <3% in 1 minute of application of the ionophore. Panels D and E illustrate results such as those in A and B, respectively, but at the electron microscope level. The macropinosome vacuoles packed with Bds (arrows in D), similar to those of Fig. 1H,I, are no longer visible after 1 minute of IONO administration (E). Bar, 0.5 μm (D), also valid for E.

vacuoles in cells not treated with Vac1, see Fig. 1H,I and Fig. 4D; $P<0.05$). All other organelles appeared normal (Fig. 6E and not shown).

In the Vac1-pretreated cells, application of IONO for 5 minutes had no large effect. With respect to the unstimulated cells the density of Bd-rich, EEA1-positive puncta (illustrated in Fig. 6B and quantified in Fig. 6D) was decreased only moderately (–15%), and non-significantly. Also, the ultrastructure of the Bd-rich vacuoles (Fig. 6F) and their Bd density (579±187 per μm^2, counted in ten vacuoles) were unchanged. We conclude that, in the experimental conditions employed (Cerny et al., 2005), Vac1 blocks the IONO-induced discharge of macropinosomes.

Macropinosome traffic is bidirectional

In view of the intense, Ca^{2+}-dependent exocytic discharges triggered by IONO, the possibility of analogous, although smaller exocytic responses induced by the two tracers, Bds and Dex, was taken into consideration. In three experiments (Fig. 7A) DCs, exposed to FITC-conjugated Bds (green) for 20 minutes in order to reach apparent loading saturation (see Fig. 1A,B), were washed and switched for 10 minutes in the same concentration of Bds, but conjugated with TRITC (red). Morphometric analysis of confocal images from two groups of 30 cells revealed that, during the second incubation, the average FITC fluorescence had decreased by over 30% ($P<0.05$), concomitantly with a similar accumulation of

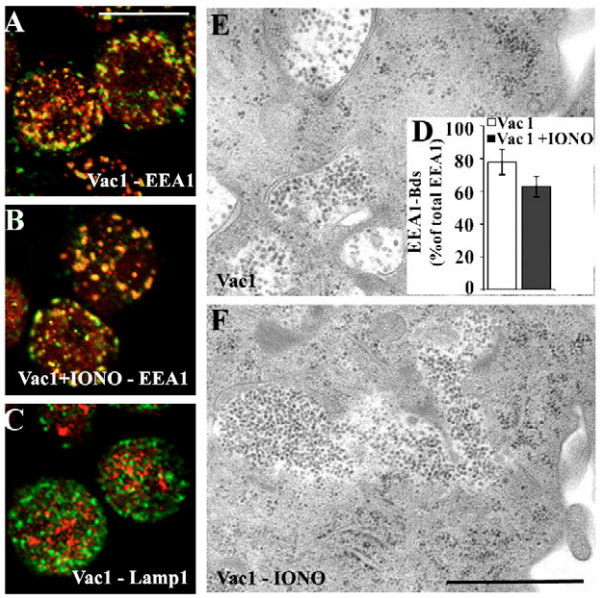

Fig. 6. Blockade by vacuolin1 of the ionomycin-induced discharge of macropinosomes. Panel A shows merged images of DCs pretreated with Vac1 and loaded for 10 minutes with Bds (green) and immunolabelled for EEA1 (red), showing extensive co-localization of the two signals (yellow) in fluorescent puncta distinctly larger than those of non-pretreated cells (Fig. 1E and Fig. 5A). Panel B shows DCs as in A but stimulated with IONO for 1 minute. The puncta positive for both Bds and EEA1 appear unaffected by the ionophore. Morphometric quantification of the data in the VAC1-pretreated cells before and after IONO (D) reveals an almost doubling of the percentage of dually positive puncta, with respect to DCs non-pretreated with the drug (Fig. 5C), and no significant decrease induced by the ionophore. At the ultrastructural level (panels E,F), the VAC1-pretreated cells show swollen macropinosomes. Their Bd density is similar in IONO-treated and untreated cells and distinctly lower than that of macropinosomes of non-pretreated DCs (Fig. 1H,I and Fig. 5D). Panel C shows VAC1-pretreated DCs loaded with Bds as in A, immunolabelled for Lamp1 (red). Lamp-1-positive puncta are larger than in non-pretreated cells, however their lack of co-localization with the tracer is as in untreated cells (supplementary material Fig. S1B,D). Bar, 10 μm (A), also valid for B and C. Bar, 0.5 μm (F), also valid for E.

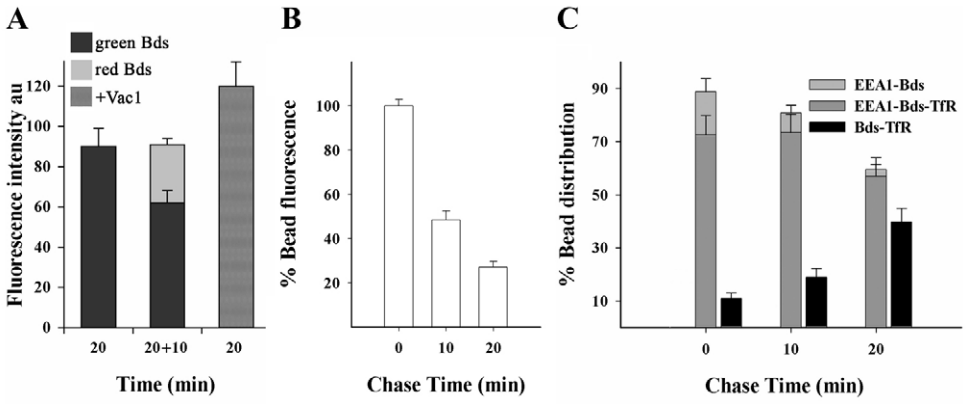

Fig. 7. Macropinocytosis-macropinosome discharge coupling. The two left histograms of panel A summarize FACS results with DCs loaded for 20 minutes with FITC-conjugated Bds and then split in two aliquots, one fixed immediately (left), the other after an additional 10 minutes of incubation with TRITC-conjugated Bds (centre). Notice the decrease of the FITC signal (over 30%) during the second incubation compensated by an analogous accumulation of the TRITC signal, indicating replacement of the discharged green Bds with red Bds. The histogram to the right of A shows that the 20 minutes of accumulation of FITC-conjugated Bds in DCs pretreated with Vac1 is almost 30% larger than that of non-pretreated cells, as expected for a drug-induced blockade of macropinosome discharge. The DCs of panels B and C, first pulsed for 20 minutes with FITC-conjugated Bds, were chased for 10 or 20 minutes with non-fluorescent Bds and then immunolabelled for EEA1 and TfR. Morphometric analyses of confocal images (at least ten fields) revealed considerable decreases of Bd fluorescence during chase (B), largely because of the discharge of Bd-rich puncta positive for EEA1 (C). By contrast, Bd-rich puncta positive for TfR alone increased proportionally (from ~10% to ~40% of the puncta present at 0 and 20 minutes of chase, respectively, panel C).

TRITC fluorescence (Fig. 7A). When the 20 minutes of FITC-Bd-uptake incubation was performed in DCs pre-incubated with the exocytic blocker, Vac1, the accumulated fluorescence was ~28% more than in control cells (Fig. 7A, 30 cells, $P<0.02$), probably because of the macropinosome-discharge block induced by the drug.

Analyses conducted in groups of 30 DCs first loaded for 10 minutes with FITC-conjugated Bds (pulse) and then switched for 10 or 30 minutes to non-fluorescent Bds (chase) revealed a progressive decline of the fluorescent puncta (Fig. 7B) accompanied by a change of their immunolabelling with anti-EEA1 antibodies. During the 20-minute chase, the puncta positive for EEA1 decreased by over 30%, whereas those negative for EE1 and positive for the recycling endosome marker, TfR, increased in percentage by approximately fourfold (Fig. 7C). These results suggest that a large fraction of the macropinosomes generated during Bd uptake is discharged by exocytosis, while only a smaller fraction, positive for TfR, is addressed to an alternative pathway and accumulates within the cell. Traffic of macropinosomes within DCs does not appear to be unidirectional, as previously believed, but bidirectional.

Exocytosis of enlargeosomes

The partial persistence of the IONO-induced FM response in DCs pretreated with Vac1 (Fig. 4D), a treatment that blocks the exocytosis of lysosomes (Cerny et al., 2005) and macropinosomes (Fig. 6), suggested the involvement of organelle(s) competent for a form of regulated exocytosis insensitive to the drug. The enlargeosome is a non-endosomal, non-lysosomal exocytic organelle insensitive to Vac1 (Cerny et al., 2004), which is expressed by DCs (Borgonovo et al., 2002). In resting Dcs, the enlargeosome marker desmoyokin/Ahnak (d/A) appeared distributed in small puncta concentrated primarily in the proximity of the cell surface, which was almost completely negative (Fig. 8A,E). One minute after application of Bds or Dex, i.e. even before the accumulation of tracer-rich puncta, d/A-immunolabelling became appreciable at the cell surface, and grew progressively during the following 20 minutes (Fig. 8G). By contrast, the large tracer-rich puncta generated during the incubation remained always d/A-negative (Fig. 8D).

In the cells exposed to Bds the surface accumulation of d/A was not decreased by pre-treatment with Vac1 (Fig. 8H), whereas it was blocked (>90%) by Wort (Fig. 8I) and BAPTA (Fig. 8J) (data from groups of ten cells each). When, instead of the tracers, DCs were exposed to IONO, an intense d/A immunolabelling appeared rapidly at the cell surface including lamellipodia (Fig. 8K). The rise of surface immunolabelling induced by 1 minute of application of the ionophore, apparently the same in control cells and in cells pretreated with Wort or Vac1 (Fig. 8L,M; quantitative data of the inset of Fig. 8M obtained from groups of ten cells), was blocked only by preloading with BAPTA (>80% decrease, not shown).

We conclude that Bds induce a prompt but moderate and prolonged enlargeosome exocytic response in DCs. This response, which is inhibited by BAPTA and Wort, could account, at least in part, for the Vac1-insensitive surface expansion observed after tracer application. By contrast, the much stronger enlargeosome exocytic response induced by IONO, although still blocked by BAPTA, was apparently unaffected by the PI3K-blocking drug.

Both macropinocytosis and enlargeosome exocytosis are stimulated by PIP3

To investigate the role of PI3K in the generation and processing of macropinosomes, DCs were treated with C6-phosphatidylinositol 3,4,5-trisphosphate (C6-PIP3), a shuttle preparation of the product (Ozaki et al., 2000), and then immunolabelled for the phosphorylated form of akt, a PI3K target kinase (Lindmo and Stenmark, 2006). Akt phosphorylation remained below detectable levels in almost all DCs treated with Bds alone (supplementary material Fig. S4B), whereas it was detectable or high-level in most DCs treated with C6-PIP3 (supplementary material Fig. S4C), pretreated or not with Wort or BAPTA (supplementary material Fig. S4D,E). By contrast, a shuttle preparation of C6-phosphatidyl inositol 4,5-bisphosphate (C6-PIP2) was without effect (not shown). We conclude that, after exogenous application, the

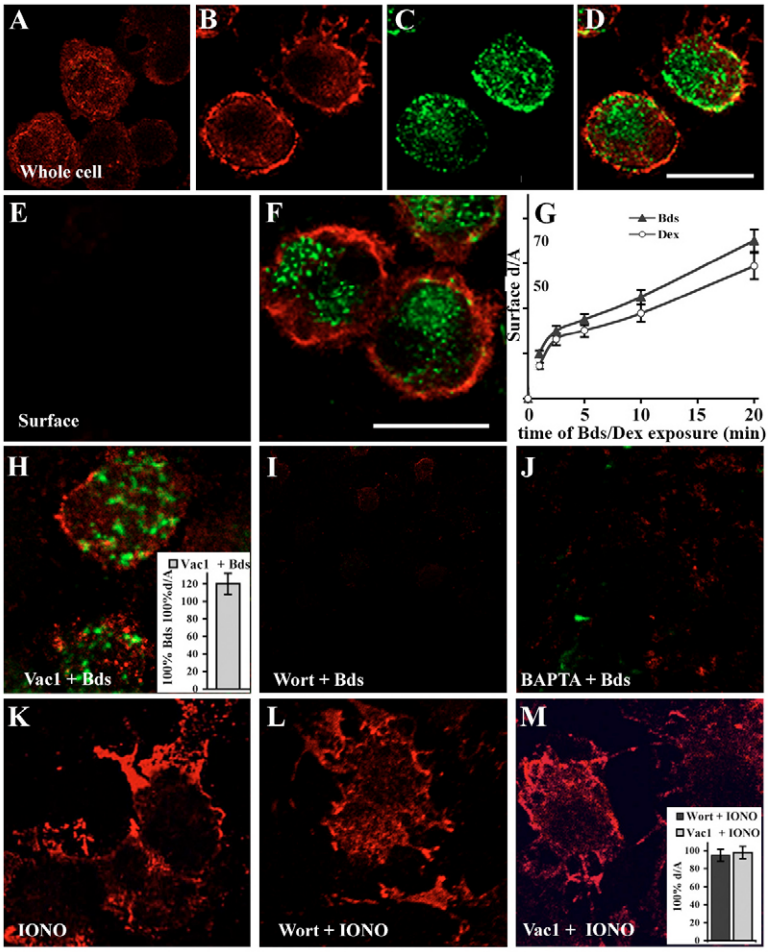

Fig. 8. Enlargeosome exocytosis in DCs exposed to the tracers or ionomycin. Panels A-D show cell images obtained from DCs permeabilized after fixation. The enlargeosome marker, d/A (red), which appears in small cytoplasmic puncta of resting DCs (A), is redistributed to the cell surface after exposure to Bds, as shown in the same cells: (B) redistribution of d/A (red); (C) the Bds taken up in 10 minutes incubation (green); (D) the merged image, which reveals the negativity for d/A of the intracellular Bd-rich puncta and the lack of coincidence of the Bds and the d/A also at the cell surface. Panels E-F and H-M show merged, red-green images of cells that were not permeabilized before immunolabelling. In these preparations, d/A (red), an enlargeosome lumenal membrane protein, is labelled only after exocytosis, at the external surface of the plasma membrane. No surface d/A signal is appreciable in resting DCs (E), whereas after Bd application (green, 10 minutes) a strong surface d/A signal becomes appreciable (F). Panel G shows the time-course of the d/A surface labelling in DCs fixed from 1 to 20 minutes after application of Bds or Dex, revealed by FACS analysis and expressed as arbitrary units. Panel H shows that the surface redistribution of d/A induced by 10 minutes of exposure to Bds was not decreased by DC pretreatment with Vac1 (quantification in ten fields), whereas it was blocked by pretreatment with Wort (panel I) and preloading with BAPTA (panel J), Panels K-M show that the d/A surface redistribution induced by IONO (K) was unaffected by pretreatment of the cells with Wort (L) or Vac1 (M). Bar, 10 μm (D), also valid for A-C. Bar, 10 μm (F) and H-M.

accumulation of PIP3 is probably much larger than that occurring in macropinocytizing cells. This difference might account for the much stronger akt phosphorylation observed in the cells loaded with PIP3 by the shuttle preparation.

We next investigated whether, in DCs pretreated with Wort or BAPTA, C6-PIP3 and C6-PIP2 relieve the inhibition of macropinocytosis and enlargeosome exocytosis. In DCs exposed to the phosphoinositide trisphosphate, uptake of Bds took place irrespective of the drug pretreatments yielding puncta, often of large size, concentrated close to the plasma membrane (Fig. 9A,B; reconstructions in supplementary material movies 1 and 2). C6-PIP3 also induced a clear surface redistribution of the enlargeosome marker d/A, both in cells exposed (Fig. 9A,B) and not exposed (Fig. 9C) to Bds. By contrast, the phosphoinositide bisphosphate had no effect on the inhibition, by BAPTA (Fig. 9D) or Wort (not shown), of either the Bd uptake or the d/A surface transfer.

In the cytoplasm of C6-PIP3-treated DCs, most of the superficial Bd-rich puncta were EEA1-negative (Fig. 9H). However, when the cells were first exposed to C6-PIP3 together with Bds and FM4-64 and then thoroughly washed, they appeared positive for the styryl dye (Fig. 9E), proving to be discrete vacuoles. Only in the cells pretreated with Wort (Fig. 9F) and, even more, with BAPTA (Fig. 9G), some of the puncta of the C6-PIP3-treated DCs failed to keep their FM4-64 staining, as expected for invaginations in continuity with the plasmalemma.

Taken together, our results suggest that in DCs challenged with C6-PIP3 the initial stages of macropinocytosis can occur. However, sealing of macropinosomes is efficient only when $[Ca^{2+}]_i$ rise and PI3K phosphorylation are not inhibited. Moreover, the large macropinosome vacuoles generated under these conditions appear defective, since they neither acquire endosomal markers nor move deep into the cytoplasm.

Discussion

Compared with phagocytosis and clathrin-dependent endocytosis, macropinocytosis is still poorly understood. In particular it is unclear whether the process is unique or not, inasmuch as it is believed to take place at a constant rate in DCs and under the stimulatory control of various intracellular signals in macrophages, lymphocytes, fibroblasts and epithelial cells. The present study, performed in human DCs, was focused on a largely unexplored area, that of membrane traffic events taking place during macropinocytosis in a time window from 0.5 to 30 minutes after application of fluorescent tracers such as small (20 nm) latex Bds or 70 kDa Dex. Multiple lines of evidence documented the macropinocytic nature of the investigated process. These included the uptake of Bds and Dex, two preferential, if not specific tracers; the inhibition not only by Wort and LY-294002, the PI3K blockers that affect all types of endocytosis, but also by amiloride, a drug that affects neither phagocytosis nor clathrin- or raft-dependent endocytosis (Geckle et al., 2001; Meier et al., 2002; Wadia et

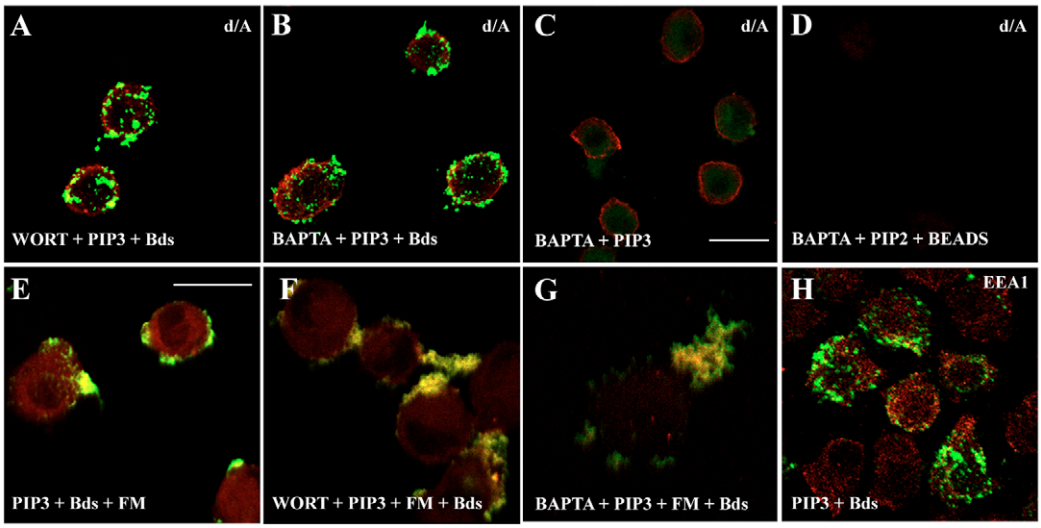

Fig. 9. Bead uptake and d/A surface redistribution in DCs exposed to PIP3. Panels A-D are merged images of DCs exposed to phosphoinositides for 20 minutes, loaded or not with the Bds for 10 minutes, fixed and surface immunolabelled for d/A. With PIP3, Bd uptake and d/A surface appearance took place even after pretreatment with Wort (A) or preloading with BAPTA (B). Notice the large size of the PIP3-induced Bd-rich puncta mostly located near the plasma membrane (tridimensional reconstruction in supplementary material Fig. S5); (compare with the cells exposed to the beads only: Fig. 1D,E; Fig. 5A, Fig. 8D,F,H). In PIP3-exposed DCs pretreated with Wort (not shown) or preloaded with BAPTA (C) the d/A surface redistribution occurred even without Bd loading. By contrast, the PIP3 precursor, PIP2, had no effect in DCs, not-pretreated and pretreated with Wort (not shown) or with BAPTA (D). Panels E-G show merged images of DCs pretreated with PIP3 as in A-C and then loaded for 10 minutes with Bds (green) together with FM4-64 (FM, red). The large Bd-rich puncta of E were sealed, discrete vacuoles because after washing they retained their FM staining. Some loss of the FM signal was visible in contrast to DCs pretreated with Wort (F) and, even more, in those preloaded with BAPTA (G). The Bd-rich puncta induced by PIP3 were negative for EEA1 (red in H). Bar, 10 μm (C), also valid for A,B,D,H. Bar, 10 μm (E), also valid for F and G.

al., 2004); and the molecular and structural features of macropinosomes. Among the new properties of the process that we have revealed, two appear particularly relevant and unexpected, concerning the rate of macropinosome generation and the exocytic recycling of macropinosomes. The former is not constant but increases considerably after tracer application, in a Ca^{2+}- and PIP3-dependent fashion; the latter, at variance with those of other endosomes, appears regulated by Ca^{2+} and can take place very fast, being completed within 1 minute when DCs are treated with a μM concentration of IONO.

The membrane traffic events taking place in DCs exposed to macropinocytic tracers are summarized in the three-phase model shown in Fig. 10. Phase 1 corresponds to the time (~4 minutes after application of the tracers) during which the rate of macropinocytosis remains low. Most likely the delay in the conversion, from low- to high-rate, was not because of the time needed for the tracers to get in contact with the cells, which was short, but rather the rise of $[Ca^{2+}]_i$ induced in the cells, which was already detectable after 1 minute but subsequently developed at a slow rate. In fact, when such a $[Ca^{2+}]_i$ rise was prevented by preloading the cells with the high-affinity Ca^{2+} chelator, BAPTA, macropinocytosis was blocked. Whether this slow $[Ca^{2+}]_i$ rise is because of a moderate increase of the cation influx across the plasma membrane or a slow release from the intracellular stores has yet to be established.

The coupling between tracer application, $[Ca^{2+}]_i$ rise and increase in macropinosome generation remains unexplained. Both Bds and Dex are known as inert tracers. Their direct activation of specific surface receptors appears therefore unlikely. Participation of other agents contained in the preparations used is also unlikely because the tracers were simply suspended in a buffer. When the latter was applied to the cells it remained without any effect on both $[Ca^{2+}]_i$ and macropinosome generation. We assume therefore that Bds and Dex, possibly after their contact with the cell and/or concentration within the first newly generated macropinosomes (de Baey and Lanzavecchia, 2000), induced the slow $[Ca^{2+}]_i$ increase through contact or osmotic interactions with the membrane. Interestingly, these events appear to occur upstream of PI3K, which is also necessary for macropinocytosis (see Amyere et al., 2000; Mellman and Steinman, 2001; Racoosin and Swanson, 1993; Araki et al., 2003; Swanson et al., 1999; Rupper et al., 2001; Lindmo and Stenmark, 2006). In fact, blocking of PI3K by Wort left the tracer-induced $[Ca^{2+}]_i$ rise unaffected.

A distinct traffic process that we have found to start in Phase 1 is the exocytosis of small cytoplasmic vesicles, the enlargeosomes (Borgonovo et al., 2002). This exocytosis, which resembles the prompt exocytosis of still uncharacterized organelles taking place in macrophages before phagosome sealing (Bajno et al., 2000; Di et al., 2003), might be a compensatory process (Morris and Homann, 2001), contributing to the DC surface area during macropinocytic internalization of the plasma membrane. Alternatively, the two processes, although triggered in a Ca^{2+}-dependent fashion, could be independent of each other, as suggested by the exclusion of the enlargeosome membrane from that of macropinosomes. The present results obtained in DCs revealed for the first time that the regulation of enlargeosome exocytosis might be dual. In fact, with low $[Ca^{2+}]_i$ increases, such as those

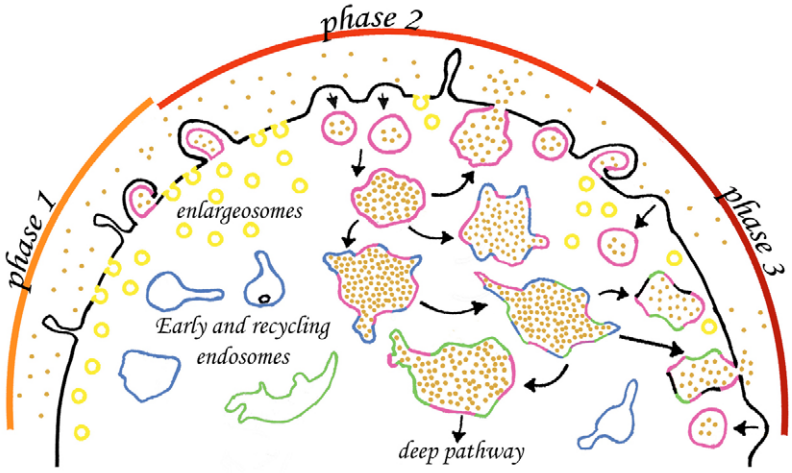

Fig. 10. Macropinocytic membrane traffic in tracer-exposed DCs. The model illustrates three sequential membrane traffic phases (specified at the top and dealt with in the Discussion), occurring in DCs during the first 30 minutes of tracer (orange dots) exposure. Phase 1 starts with the application of the tracers (Bds or Dex) and ends 4 minutes later, with the change of the kinetics of tracer uptake (see Fig. 2A). During this time $[Ca^{2+}]_i$ begins to rise in DCs (see Fig. 3D,E). In addition to the low-rate macropinocytosis, the main traffic event of Phase 1 is the early exocytosis of enlargeosomes (yellow membrane), initiated within 1 minute and continued thereafter (see Fig. 8G). Some specialization of the plasma membrane by sorting of specific components, anticipating the generation of macropinosomes (purple), is assumed to take place at the bending ruffles sticking out from the cell surface. The increased rate of tracer-positive macropinosome (purple membrane) generation, which seems to depend on $[Ca^{2+}]_i$ (blocked by cell preloading with BAPTA) and PI3K activity (blocked by Wort) (see Fig. 2 and supplementary material Fig. S2), is illustrated in Phase 2. Macropinosomes, progressively enlarged (probably by fusion) and packed with the tracer, acquire in sequence various markers: first Rbk-5, then EEA1 (early endosomes, blue membrane) and finally TfR (recycling endosomes, green membrane) (Fig. 2B,C; supplementary material Fig. S2). During this phase tracer uptake predominates, however macropinosomes can undergo regulated exocytosis (regurgitation, blocked by Vac1, Fig. 7A), with discharge of their segregated tracer. This process depends on $[Ca^{2+}]_i$. In the case of μM $[Ca^{2+}]_i$ increases, such as those induced by IONO, exocytosis becomes prompt and complete (see Fig. 5). The alternative possibility, more frequent for macropinosomes positive for TfR and no longer for EEA1 (Fig. 7C), is entering in a 'deep pathway', presumably leading to processing and finally to presentation of the antigens. Phase 3, in which uptake and discharge of tracer approach equilibrium, begins after ~20 minutes of application (Fig. 1B and Fig. 7) and probably continues as long as the tracer is applied. During this phase, even if macropinocytosis continues at similar rate, the number of macropinosomes per DC remains approximately stable (Fig. 1A,B and Fig. 7A) so that cell overloading is prevented.

induced by the tracers, PI3K activity was necessary as shown by the Wort inhibition of the exocytic responses. By contrast, at high $[Ca^{2+}]_i$ by IONO administration, or at high PIP3 by application of the membrane-permeant C6-PIP3, enlargeosome exocytosis was stimulated even when PI3K was inhibited by Wort or $[Ca^{2+}]_i$ rise buffered by BAPTA, respectively.

Phase 2 of Fig. 10 (between ~4 and 20 minutes of tracer application) begins with the increase of the macropinosome generation rate and proceeds until a quasi-equilibrium is reached in terms of tracer traffic to and from the plasma membrane. Several important processes take place in newly generated macropinosomes. They first acquire Rbk, a marker specific for macropinosomes and for a subpopulation of early endosomes, and then EEA1, the classical early endosome marker. These acquisitions are probably because of molecular changes of the macropinosome membrane, with ensuing binding of the specific protein complexes, including either one or both markers, associated to their cytosolic surface. TfR, a transmembrane protein, is acquired later, most likely by fusion of macropinosomes with bona fide endosomes. Of these processes, which had already been described (Hewlett et al., 1994; Schnatwinkel et al., 2004), we have detailed timing and extent. Moreover, we have shown that the macropinosomes generated in response to application of C6-PIP3, and not of the tracers, failed to proceed from their early stage to that positive for endosome markers. As yet unidentified signals might therefore be needed to regulate this maturation step.

Macropinosomes are not simple endosomes. Although sharing common markers, they in fact do not intermix, but coexist as an at least partially distinct organelle subpopulation (see Hewlett et al., 1994). Endosomes are known to recycle continuously, from both their early and recycling pools to the plasma membrane (Sheff et al., 1999), although by constitutive exocytosis (Maxfield and McGraw, 2004; Knight, 2002). In the case of macropinosomes, some recycling had also been shown, but in cells other than DCs, and its regulation had not been investigated (Veithen et al., 1998; Hamasaki et al., 2004). Our results demonstrate that macropinosome recycling also occurs in DCs, as documented by the results of our tracer pulse-chase experiments. In addition, such a recycling is not constitutive, but Ca^{2+}-regulated. Ca^{2+}, therefore, plays an unexpected dual role in macropinocytosis: it is necessary both for the generation of the organelles and for their continuous recycling. Moreover, when $[Ca^{2+}]_i$ rises to the μM level the latter process increases strongly. Therefore, in case of an intense DC stimulation, the macropinocytized cargo, diverted from its intracellular pathway, can be rapidly regurgitated into the extracellular space.

Vac1 is a drug initially proposed as a blocker of the regulated exocytosis of lysosomes (Cerny et al., 2004). Recently, however, this action has been questioned (Huynh and Andrews, 2005). Working on DCs pretreated with Vac1 (Cerny et al., 2005) and stimulated with IONO, we have now shown that the IONO-induced exocytosis of macropinosomes is also blocked by the drug, whereas that of enlargeosomes is not. Regulated exocytoses of macropinosomes and lysosomes therefore appear to share at least some properties that are not common to enlargeosome exocytosis.

Phase 3 of Fig. 10, which begins with the quasi-equilibration between macropinocytosis and exocytosis (~20 minutes of tracer application), is able to proceed as long as the incubation of DCs with the tracers is pursued. During this phase only a minor fraction of macropinosomes appears to proceed along the endosomal pathway, while the rest are continuously exocytized.

From a functional point of view the macropinocytosis-exocytosis coupling might come across as a futile cycle. The present data and those by others (Hewlett et al., 1994; Schnatwinkel et al., 2004) show, however, that during their intracellular life macropinosome membranes change their properties. Also, the cargo molecules are processed and might be segregated from each other, at least partially, beginning with water loss (de Baey and Lanzavecchia, 2000) and an ensuing volume reduction. Therefore, the organelles discharged by exocytosis are quite different from those initially generated by macropinocytosis. The macropinocytosis-exocytosis coupling might allow DCs to keep scanning the medium for solutes and solid materials even when their macropinocytic rate is high, with no risk of overloading their cytoplasm with macropinosomes.

In conclusion, DC macropinocytosis appears as a regulated, Ca^{2+}- and PIP3-dependent process involving the coordinated traffic of various types of membranes aimed at a variety of tasks. These include the uptake of cargo from the extracellular space, the preservation of the surface membrane area, and the regulation of membrane traffic along the intracellular pathway and of cell loading with macropinosomes.

Materials and Methods

Materials

The antibodies and reagents used were as follows: mouse monoclonal anti-d/A (Borgonovo et al., 2002) and anti-calreticulin (Cocucci et al., 2004) from the Meldolesi laboratory; rabbit polyclonal anti-rabankyrin-5 (Rbk), a gift of M. Zerial (MPI for Molecular Cell Biology and Genetics, Dresden, Germany); rabbit polyclonal anti-EEA1 (Affinity Bioreagents, Golden, CO); monoclonal anti-Lamp1 (mouse), anti-EEA1 (human), anti-HLA-DR (human), and recombinant human IL-4 (BD Transduction Laboratories, San Diego, CA); monoclonal anti-TfR (mouse) (Zymed Laboratories, San Francisco, CA); rabbit polyclonal anti-akt (Cell Signalling, Beverly, MA); goat TRITC-labelled and Cy5-labelled anti-rabbit and anti-mouse IgG (Jackson ImmunoResearch Laboratories, Bar Harbor, MA); goat anti-mouse IgG and goat anti-mouse IgG-coated magnetic Dynabeads M-450 (Dynal, Oslo, Norway); recombinant human GM-CSF (Schering Plough, Milan, Italy); Fycoll-Paque (BioChrom, Berlin, Germany); polystyrene-carboxylate microspheres (i.e. latex Bds) 20 nm in diameter, conjugated with FITC, TRITC and unconjugated; Dex 70 kDa conjugated with FITC; transferrin (Tf) conjugated with TRITC, fura-2-AM, FM1-43, FM4-64, C6-PIP3, C6-PIP2, and BAPTA-AM (Molecular Probes, Eugene, OR); Percoll (Amersham Bioscience, Little Chalfont, UK); saponin (Calbiochem EMD Bioscience, San Diego, CA); unconjugated 70 kDa Dex, wortmannin (Wort), LY-294002 and LY-303511, amiloride and ionomycin (IONO) (Sigma-Aldrich, St Louis, MO); vacuolin1 (Vac1) (the Kirchhausen laboratory); reagents for cell culture [Life Technologies, except fetal calf serum (FCS) (clone III) (Hyclone-Cellbio, Milan, Italy)].

Preparation of immature DCs

Mononuclear cells from healthy donors were isolated from buffy coats. For separation on Fycoll-Paque gradient (Paolucci et al., 2000), the cells (in RPMI 1640 containing 10% FCS, 2 mM glutamine, penicillin and streptomycin) were transferred, for 1 hour at 37°C, to six-well plates (Costar, Cambridge, MA). Adherent cells were cultured (5 days) in the above medium supplemented with human GM-CSF (50 ng/ml) and IL-4 (1000 U/ml). Residual T cells were removed by binding to mouse anti-CD3 monoclonal antibodies (1 μg/10^6 cells) and goat anti-mouse IgG-coated Dyna beads M-450 (Paolucci et al., 2003). Preparations containing >1% residual lymphocytes were discarded.

Drugs and agents

The following chemicals, dissolved in dimethylsulfoxide (DMSO), were diluted in culture medium and administered to DCs at the indicated times before Bd administration: BAPTA-AM, 30 μM, 30 minutes; Wort, 300 nM, 1 hour; LY-294002 and LY-303511 25 μM, 30 minutes; Vac1, 1 μM, 2 hours; amiloride, 3 mM, 15 minutes. IONO was administered at 3 μM. Controls received the same volume of DMSO dissolved in the medium, but with no drugs. PIP3 and PIP2 (1 μg/μl), dissolved in water, were mixed with shuttle PIP1 (0.5 mM) to form complexes (Ozaki et al., 2000) and added to DC suspensions. All solutions employed scored negative when assessed for endotoxin contamination by the Lymulus gelification test (PBI, Milan, Italy).

Macropinocytosis

Latex Bds (20 nm in diameter, conjugated with FITC, TRITC or unconjugated) sonicated for 5 minutes and kept on ice for 20 minutes, and 70 kDa Dex (conjugated with FITC or unconjugated) suspended in PBS were administered to DC suspensions in culture medium (final Bds:DC ratio, 5×10^6; Dex concentration, 2.5 mg/ml). Incubations at 37°C were for 0.5-30 minutes, after which cells were washed twice with cold PBS by centrifugation at 150 ***g***, and then processed as reported in cytofluorescence and immunofluorescence.

Fluorescence-activated cell sorting (FACS) analysis

DC suspensions loaded with tracers were washed twice with ice-cold PBS and then fixed with 4% paraformaldehyde in PBS, pH 7.4 (5°C for 10 minutes). After quenching with 0.1 M glycine and washing first with PBS containing 0.1% bovine serum albumin (BSA) and 10% goat serum, then with plain medium, they were resuspended at 10^6/ml in PBS, and analyzed by FACS (Paolucci et al., 2003).

Cytofluorescence and immunofluorescence

DCs, loaded with or without the tracers, were resuspended in 100 μl of PBS (2×10^5/ml), cytospun for 4 minutes at 170 ***g***, fixed for 10 minutes with 4% formaldehyde in PBS, quenched and washed as for FACS, then either analyzed for cytofluorescence (Lutz et al., 1997) or processed for immunofluorescence. For whole-cell immunolabelling, coverslips were covered with PBS-BSA-goat serum containing 0.1% saponin (30 minutes), then washed, exposed to the primary antibodies in the saponin-containing solution (1.5 hours, 22°C), extensively washed, exposed to the secondary antibodies (TRITC- or Cy5-conjugated) in the same solution (1.5 hours, 22°C), and finally washed and mounted. For surface immunolabelling the protocol was the same, however the solutions contained no saponin and therefore the cells were not permeabilized. Samples were analyzed with the BioRad MRC 1024 and Leica SP2 AOBs confocal microscopes.

For morphometric analyses the confocal images, acquired at constant parameters of illumination and gain, were analyzed quantitatively by using the ImageJ software program. Specifically, the fluorescence intensity above the threshold of each pixel in the image, fixed to cut off the background signal, was measured at one-, two- or three wavelengths to map quantitatively the distribution of single-, two- or three markers (Cocucci et al., 2004). Statistical significance was established by the Student's *t*-test. For tridimensional reconstructions, optical sections, taken every 150 nm with a wide-field microscope on the Delta Vision system, were analyzed by the soft WoRx Deconvolve software (Applied Precision, Issaquah, WA).

$[Ca^{2+}]_i$ assays

Washed cell suspensions (1×10^6/ml in Krebs-Ringer Hepes (KRH) medium containing 125 mM NaCl, 5 mM KCl, 1 mM $MgSO_4$, 1 mM $KH2PO_4$, 25 mM HEPES, 1 mM $CaCl_2$, 6 mM glucose) were incubated with fura-2-AM (5 μM, 37°C, 30 minutes). One ml washed samples were transferred to a warm conditioned cuvette in a LS50B fluorimeter (Perkin Elmer, Wellesley, MA). The ratiometric 340/380 nm excitation signals were recorded under continuous stirring. Results are given as $\Delta R/R_o$, where R_o is the ratio value in resting cells. Calculations of $[Ca^{2+}]_i$ were made as in Cocucci et al. (Cocucci et al., 2004).

FM dyes in single cells and cell suspensions

DC suspensions in KRH, supplemented with either FM1-43 or FM4-64 dyes (4 μM), were exposed or not to the tracers for the times indicated in the text and figures, then extensively washed, cytospun and mounted while unfixed. The preparations were then analyzed in the confocal microscope for the fluorescence of intracellular membranes that during incubation with the dye had been in continuity with the plasma membrane. Other suspensions were transferred to the fluorimeter, and FM dyes were added under continuous stirring. After at least 5 minutes, necessary for dye diffusion and equilibration in the plasma membrane, IONO was added, and the increases in fluorescence intensity, proportional to the enlargements of the plasma membrane as a consequence of exocytoses, were recorded on-line (excitation and emission wavelengths: 479 nm and 598 nm for FM1-43; 500 nm and 700 nm for FM4-64) (van der Wijk et al., 2003).

Electron microscopy

DC suspensions were centrifuged and the pellets, fixed with 4% paraformaldehyde-2% glutaraldehyde in PBS (30 minutes) and postfixed (1 hour) with 1% OsO_4 in PBS, were washed and embedded in Epon. Conventional thin sections were collected on uncoated grids, stained with uranyl acetate and lead citrate and examined in a Hitachi H7000 electron microscope (Hitachi, Tokyo Japan). Latex Bds segregated within macropinosomes of randomly chosen prints were counted as indicated in the text.

We thank F. Floriani for assistance, and M. Zerial for the gift of the anti-rabakyrin-5 antibody. This work was supported in part by grants from the Italian Association for Cancer Research (AIRC) to E.C., Telethon Fondazione ONLUS (GGP030234), the European Community (APOPIS-LSHM-CT-2003-503330), and the FIRB 2004 Programme of the Italian Ministry of Research (MIUR) to J.M.

References

Amyere, M., Payrastre, B., Krause, U., Van Der Smissen, P., Veithen, A. and Courtoy, P. J. (2000). Constitutive macropinocytosis in oncogene-transformed fibroblasts depends on sequential permanent activation of phosphoinositide 3-kinase and phospholipase C. *Mol. Biol. Cell* **11**, 3453-3467.

Amyere, M., Mettlen, M., Van Der Smissen, P., Platek, A., Payrastre, B., Veithen, A. and Courtoy, P. J. (2002). Origin, originality, functions, subversions and molecular signalling of macropinocytosis. *Int. J. Med. Microbiol.* **291**, 487-494.

Araki, N., Johnson, M. T. and Swanson, J. A. (1996). A role for phosphoinositide 3-kinase in the completion of macropinocytosis and phagocytosis by macrophages. *J. Cell Biol.* **135**, 1249-1260.

Araki, N., Hatae, T., Furukawa, A. and Swanson, J. A. (2003). Phosphoinositide-3-kinase-independent contractile activities associated with Fcgamma-receptor-mediated phagocytosis and macropinocytosis in macrophages. *J. Cell Sci.* **116**, 247-257.

Bajno, L., Peng, X. R., Schreiber, A. D., Moore, H. P., Trimble, W. S. and Grinstein, S. (2000). Focal exocytosis of VAMP3-containing vesicles at sites of phagosome formation. *J. Cell Biol.* **149**, 697-706.

Borgonovo, B., Cocucci, E., Racchetti, G., Podini, P., Bachi, A. and Meldolesi, J. (2002). Regulated exocytosis: a novel, widely expressed system. *Nat. Cell Biol.* **4**, 955-962.

Cerny, J., Feng, Y., Yu, A., Miyake, K., Borgonovo, B., Klumperman, J., Meldolesi, J., McNeil, P. L. and Kirchhausen, T. (2004). The small chemical vacuolin-1 inhibits Ca(2+)-dependent lysosomal exocytosis but not cell resealing. *EMBO Rep.* **5**, 883-888.

Cerny, J., Feng, Y., Yu, A., Miyake, K., Borgonovo, B., Klumperman, J., Meldolesi, J., McNeil, P. L. and Kirchhausen, T. (2005). Corrigendum: The small chemical vacuolin-1 inhibits Ca(2+)-dependent lysosomal exocytosis but not cell resealing. *EMBO Rep.* **9**, 898.

Cochilla, A. J., Angleson, J. K. and Betz, W. J. (1999). Monitoring secretory membrane with FM1-43 fluorescence. *Annu. Rev. Neurosci.* **22**, 1-10.

Cocucci, E., Racchetti, G., Podini, P., Rupnik, M. and Meldolesi, J. (2004). Enlargeosome, an exocytic vesicle resistant to nonionic detergents, undergoes endocytosis via a nonacidic route. *Mol. Biol. Cell* **15**, 5356-5368.

de Baey, A. and Lanzavecchia, A. (2000). The role of aquaporins in dendritic cell macropinocytosis. *J. Exp. Med.* **191**, 743-748.

Dharmawardhane, S., Schurmann, A., Sells, M. A., Chernoff, J., Schmid, S. L. and Bokoch, G. M. (2000). Regulation of macropinocytosis by p21-activated kinase-1. *Mol. Biol. Cell* **11**, 3341-3352.

Di, A., Nelson, D. J., Bindokas, V., Brown, M. E., Libunao, F. and Palfrey, H. C. (2003). Dynamin regulates focal exocytosis in phagocytosing macrophages. *Mol. Biol. Cell* **14**, 2016-2028.

Ellerbroek, S. M., Wennerberg, K., Arthur, W. T., Dunty, J. M., Bowman, D. R., DeMali, K. A., Der, C. and Burridge, K. (2004). SGEF, a RhoG guanine nucleotide exchange factor that stimulates macropinocytosis. *Mol. Biol. Cell* **15**, 3309-3319.

Fiorentini, C., Falzano, L., Fabbri, A., Stringaro, A., Logozzi, M., Travaglione, S., Contamin, S., Arancia, G., Malorni, W. and Fais, S. (2001). Activation of rho GTPases by cytotoxic necrotizing factor 1 induces macropinocytosis and scavenging activity in epithelial cells. *Mol. Biol. Cell* **12**, 2061-2073.

Garrett, W. S., Chen, L. M., Kroschewski, R., Ebersold, M., Turley, S., Trombetta, S., Galan, J. E. and Mellman, I. (2000). Developmental control of endocytosis in dendritic cells by Cdc42. *Cell* **102**, 325-334.

Gekle, M., Freudinger, R. and Mildenberger, S. (2001). Inhibition of Na+-H+ exchanger-3 interferes with apical receptor-mediated endocytosis via vesicle fusion. *J. Physiol.* **531**, 619-629.

Hamasaki, M., Araki, N. and Hatae, T. (2004). Association of early endosomal autoantigen 1 with macropinocytosis in EGF-stimulated A431 cells. *Anat. Rec. A Discov. Mol. Cell Evol. Biol.* **277**, 298-306.

Harding, C. V. and Geuze, H. J. (1992). Class II MHC molecules are present in macrophage lysosomes and phagolysosomes that function in the phagocytic processing of Listeria monocytogenes for presentation to T cells. *J. Cell Biol.* **119**, 531-542.

Henson, P. M., Bratton, D. L. and Fadok, V. A. (2001). Apoptotic cell removal. *Curr. Biol.* **11**, R795-R805.

Hewlett, L. J., Prescott, A. R. and Watts, C. (1994). The coated pit and macropinocytic pathways serve distinct endosome populations. *J. Cell Biol.* **124**, 689-703.

Huynh, C. and Andrews, N. W. (2005). The small chemical vacuolin-1 alters the morphology of lysosomes without inhibiting Ca2+-regulated exocytosis. *EMBO Rep.* **6**, 843-847.

Knight, D. E. (2002). Calcium-dependent transferrin receptor recycling in bovine chromaffin cells. *Traffic* **3**, 298-307.

Kolb-Maurer, A., Wilhelm, M., Weissinger, F., Brocker, E. B. and Goebel, W. (2002). Interaction of human hematopoietic stem cells with bacterial pathogens. *Blood* **100**, 3703-3709.

Kruth, H. S., Jones, N. L., Huang, W., Zhao, B., Ishii, I., Chang, J., Combs, C. A., Malide, D. and Zhang, W. Y. (2005). Macropinocytosis is the endocytic pathway that mediates macrophage foam cell formation with native low density lipoprotein. *J. Biol. Chem.* **280**, 2352-2360.

Lanzetti, L., Palamidessi, A., Areces, L., Scita, G. and Di Fiore, P. P. (2004). Rab5 is a signalling GTPase involved in actin remodelling by receptor tyrosine kinases. *Nature* **429**, 309-314.

Lindmo, K. and Stenmark, H. (2006). Regulation of membrane traffic by phosphoinositide 3-kinases. *J. Cell Sci.* **119**, 605-614.

Lutz, M. B., Rovere, P., Kleijmeer, M. J., Rescigno, M., Assmann, C. U., Oorschot, V. M., Geuze, H. J., Trucy, J., Demandolx, D., Davoust, J. et al. (1997). Intracellular routes and selective retention of antigens in mildly acidic cathepsin D/lysosome-associated membrane protein-1/MHC class II-positive vesicles in immature dendritic cells. *J. Immunol.* **159**, 3707-3716.

Maxfield, F. R. and McGraw, T. E. (2004). Endocytic recycling. *Nat. Rev. Mol. Cell Biol.* **5**, 121-132.

Meier, O. and Greber, U. F. (2004). Adenovirus endocytosis. *J. Gene Med.* **6**, S152-S163.

Meier, O., Boucke, K., Hammer, S. V., Keller, S., Stidwill, R. P., Hemmi, S. and Greber, U. F. (2002). Adenovirus triggers macropinocytosis and endosomal leakage together with its clathrin-mediated uptake. *J. Cell Biol.* **158**, 1119-1131.

Mellman, I. and Steinman, R. M. (2001). Dendritic cells: specialized and regulated antigen processing machines. *Cell* **106**, 255-258.

Morris, C. E. and Homann, U. (2001). Cell surface area regulation and membrane tension. *J. Membr. Biol.* **179**, 79-102.

Muro, S., Wiewrodt, R., Thomas, A., Koniaris, L., Albelda, S. M., Muzykantov, V. R. and Koval, M. (2003). A novel endocytic pathway induced by clustering endothelial ICAM-1 or PECAM-1. *J. Cell Sci.* **116**, 1599-1609.

Ozaki, S., DeWald, D. B., Shope, J. C., Chen, J. and Prestwich, G. D. (2000). Intracellular delivery of phosphoinositides and inositol phosphates using polyamine carriers. *Proc. Natl. Acad. Sci. USA* **97**, 11286-11291.

Paolucci, C., Rovere, P., De Nadai, C., Manfredi, A. A. and Clementi, E. (2000). Nitric oxide inhibits the tumor necrosis factor alpha-regulated endocytosis of human dendritic cells in a cyclic GMP-dependent way. *J. Biol. Chem.* **275**, 19638-19644.

Paolucci, C., Burastero, S. E., Rovere-Querini, P., De Palma, C., Falcone, S., Perrotta, C., Capobianco, A., Manfredi, A. A. and Clementi, E. (2003). Synergism of nitric oxide and maturation signals on human dendritic cells occurs through a cyclic GMP-dependent pathway. *J. Leukoc. Biol.* **73**, 253-262.

Pelkmans, L. and Helenius, A. (2003). Insider information: what viruses tell us about endocytosis. *Curr. Opin. Cell Biol.* **15**, 414-422.

Racoosin, E. L. and Swanson, J. A. (1993). Macropinosome maturation and fusion with tubular lysosomes in macrophages. *J. Cell Biol.* **121**, 1011-1020.

Reece, J. C., Vardaxis, N. J., Marshall, J. A., Crowe, S. M. and Cameron, P. U. (2001). Uptake of HIV and latex particles by fresh and cultured dendritic cells and monocytes. *Immunol. Cell Biol.* **79**, 255-263.

Rupper, A., Lee, K., Knecht, D. and Cardelli, J. (2001). Sequential activities of phosphoinositide 3-kinase, PKB/Akt, and Rab7 during macropinosome formation in Dictyostelium. *Mol. Biol. Cell* **12**, 2813-2824.

Sallusto, F., Cella, M., Danieli, C. and Lanzavecchia, A. (1995). Dendritic cells use macropinocytosis and the mannose receptor to concentrate macromolecules in the major histocompatibility complex class II compartment: downregulation by cytokines and bacterial products. *J. Exp. Med.* **182**, 389-400.

Salter, R. D., Tuma-Warrino, R. J., Hu, P. Q. and Watkins, S. C. (2004). Rapid and extensive membrane reorganization by dendritic cells following exposure to bacteria revealed by high-resolution imaging. *J. Leukoc. Biol.* **75**, 240-243.

Schnatwinkel, C., Christoforidis, S., Lindsay, M. R., Uttenweiler-Joseph, S., Wilm, M., Parton, R. G. and Zerial, M. (2004). The Rab5 effector Rabankyrin-5 regulates and coordinates different endocytic mechanisms. *PLoS Biol.* **2**, E261.

Sheff, D. R., Daro, E. A., Hull, M. and Mellman, I. (1999). The receptor recycling pathway contains two distinct populations of early endosomes with different sorting functions. *J. Cell Biol.* **145**, 123-139.

Steinman, R. M. and Swanson, J. (1995). The endocytic activity of dendritic cells. *J. Exp. Med.* **182**, 283-288.

Sun, P., Yamamoto, H., Suetsugu, S., Miki, H., Takenawa, T. and Endo, T. (2003). Small GTPase Rah/Rab34 is associated with membrane ruffles and macropinosomes and promotes macropinosome formation. *J. Biol. Chem.* **278**, 4063-4071.

Swanson, J. A. and Watts, C. (1995). Macropinocytosis. *Trends Cell Biol.* **5**, 424-428.

Swanson, J. A., Johnson, M. T., Beningo, K., Post, P., Mooseker, M. and Araki, N. (1999). A contractile activity that closes phagosomes in macrophages. *J. Cell Sci.* **112**, 307-316.

Terebiznik, M. R., Vieira, O. V., Marcus, S. L., Slade, A., Yip, C. M., Trimble, W. S., Meyer, T., Finlay, B. B. and Grinstein, S. (2002). Elimination of host cell PtdIns(4,5)P(2) by bacterial SigD promotes membrane fission during invasion by Salmonella. *Nat. Cell Biol.* **4**, 766-773.

van der Wijk, T., Tomassen, S. F., Houtsmuller, A. B., de Jonge, H. R. and Tilly, B. C. (2003). Increased vesicle recycling in response to osmotic cell swelling. Cause and consequence of hypotonicity-provoked ATP release. *J. Biol. Chem.* **278**, 40020-40025.

Veithen, A., Amyere, M., Van Der Smissen, P., Cupers, P. and Courtoy, P. J. (1998). Regulation of macropinocytosis in v-Src-transformed fibroblasts: cyclic AMP selectively promotes regurgitation of macropinosomes. *J. Cell Sci.* **111**, 2329-2335.

Wadia, J. S., Stan, R. V. and Dowdy, S. F. (2004). Transducible TAT-HA fusogenic peptide enhances escape of TAT-fusion proteins after lipid raft macropinocytosis. *Nat. Med.* **10**, 310-315.

West, M. A., Bretscher, M. S. and Watts, C. (1989). Distinct endocytotic pathways in epidermal growth factor-stimulated human carcinoma A431 cells. *J. Cell Biol.* **109**, 2731-2739.

West, M. A., Prescott, A. R., Eskelinen, E. L., Ridley, A. J. and Watts, C. (2000). Rac is required for constitutive macropinocytosis by dendritic cells but does not control its downregulation. *Curr. Biol.* **10**, 839-848.

West, M. A., Wallin, R. P., Matthews, S. P., Svensson, H. G., Zaru, R., Ljunggren, H. G., Prescott, A. R. and Watts, C. (2004). Enhanced dendritic cell antigen capture via toll-like receptor-induced actin remodeling. *Science* **305**, 1153-1157.

Yang, Z., Vadlamudi, R. K. and Kumar, R. (2005). Dynein light chain 1 phosphorylation controls macropinocytosis. *J. Biol. Chem.* **280**, 654-659.